ACADEMIC PRESS

Available online at www.sciencedirect.com
SCIENCE DIRECT®

Journal of Catalysis 214 (2003) 8–14

JOURNAL OF CATALYSIS

www.elsevier.com/locate/jcat

Enhancement of the catalytic activities in propane oxidation and H–D exchangeability of hydroxyl groups by the incorporation with cobalt into strontium hydroxyapatite

Shigeru Sugiyama,* Tomotaka Shono, Daisaku Makino, Toshihiro Moriga, and Hiromu Hayashi

Department of Chemical Science and Technology, Faculty of Engineering, The University of Tokushima, Minamijosanjima, Tokushima 770-8506, Japan

Received 3 April 2002; revised 3 October 2002; accepted 7 November 2002

Abstract

The oxidative dehydrogenation of propane to propylene on strontium and cobalt–strontium hydroxyapatites (SrHAp and Co–SrHAp, respectively) and H–D exchangeability of hydroxyl groups in those catalysts with D_2O have been studied. Both the yield of C_3H_6 and H–D exchangeability were found to be enhanced with increasing the cobalt contents in the catalysts, the latter of which was investigated by solid state ^1H MAS MNR at 25 kHz. It is suggested that oxygen species, like lattice oxygen in oxide catalysts, as formed from hydrogen desorption from OH groups in the hydroxyapatites, may contribute to the activation of C_3H_8. The structure of Co–SrHAp, of which the XRD pattern was identical to that of SrHAp, was also identified with extended X-ray absorption fine structure (XAFS) and solid state ^{31}P MAS NMR.

Keywords: Oxidative dehydrogenation of propane; Deuteration; Heavy water; Cobalt–strontium hydroxyapatites

1. Introduction

The partial oxidation and oxidative dehydrogenation of alkanes to value-added products over various hydroxyapatite catalysts have been extensively studied in our laboratory. Hydroxyapatite $[M_{10}(PO_4)_6(OH)_2]$, where M is a divalent metal cation, has a hexagonal structure and is evidently a solid of considerable flexibility in its elemental composition and the hydroxyl groups can be easily exchanged by Cl^- to form the corresponding chlorapatite $[M_{10}(PO_4)_6Cl_2]$ [1,2]. Although the favorable catalytic activities for the oxidation of alkanes were found on hydroxyapatites containing calcium [3], strontium [4], and barium [5] and those incorporated with lead [6,7], rather low activities were observed on the corresponding chlorapatites [3–7]. Since the exchange of OH^- by Cl^- in those hydroxyapatites resulted in a great decrease of the activities [3–7], the active site on the hydroxyapatite appears to be OH^- groups. However, it is rather strange that OH^- groups may directly contribute to hydrogen abstraction from alkanes. It has been reported that hydrogen in the hydroxyl groups can be exchanged with deuterium in D_2O and CH_3OD [8–10]. Recently, the H–D exchangeability of the OH^- groups with CH_3OD was reconfirmed in our laboratories [11,12], indicating that oxygen species, suggested as active sites for the oxidation of alkanes on oxide catalysts, may be formed during the H–D exchange [13]. It may be reasonable that the increase of the H–D exchangeability in the hydroxyapatites results in the enhancement of the formation of such an active oxygen species to directly contribute to hydrogen abstraction from alkanes in the oxidation.

In the present paper, we report the oxidative dehydrogenation of propane on strontium hydroxyapatite and that incorporated with cobalt cation (SrHAp and Co–SrHAp, respectively) and H–D exchange behaviours of hydroxyl groups in those catalysts with D_2O. Furthermore, the structure of Co–SrHAp has been characterized by X-ray diffraction (XRD), ^{31}P and ^1H MAS NMR, and X-ray absorption spectroscopy (XAFS).

* Corresponding author.
E-mail address: sugiyama@chem.tokushima-u.ac.jp (S. Sugiyama).

0021-9517/03/$ – see front matter
doi:10.1016/S0021-9517(02)00101-X

Table 1
Preparation conditions, composition, and surface of fresh SrHAp and Co–SrHAp

Catalyst	SrHAp[a]	Co conc.[b]	Time[c]	Sr/P[d]	10^2Co/Sr[d]	SA[e]
SrHAp	20	0 mmol/150 mL	4 h	1.53 (1.52)	0 (0)	59.6
Co36SrHAp	13	46.1 mmol/100 mL	6 min	1.56 (1.47)	3.63 (14.3)	56.0
Co55SrHAp	15	51.9 mmol/150 mL	8 h	1.40 (1.45)	5.47 (16.3)	56.1

Values in parentheses were obtained by XPS.
[a] Weight of SrHAp employed (g).
[b] Initial concentration of cobalt and volume of solution employed.
[c] Duration of incorporation (h).
[d] Atomic ratio by ICP except those in parentheses.
[e] BET surface area (m^2/g).

2. Experimental

2.1. Catalyst preparation

Strontium hydroxyapatite was prepared from $Sr(NO_3)_2$ (Wako Pure Chemicals, Osaka) and $(NH_4)_2HPO_4$ (Wako) [4,7]. Cobalt cations were incorporated into the hydroxyapatite by stirring the solid and $Co(NO_3)_2 \cdot 6H_2O$ in aqueous solution at 293 K under the conditions given in Table 1 [14]. To control the amount of Co^{2+} incorporated, stirring times were adjusted to 6 min and 8 h since it is generally accepted that the incorporation of divalent cations into hydroxyapatites proceeded greatly at a rather shorter stirring time [14]. Undoped catalyst (denoted as SrHAp) was treated in the same manner but without the addition of cobalt nitrate. After being washed with water and dried at 373 K overnight, the sample after calcination at 773 K for 3 h was referred to as the "fresh catalyst." All catalysts were sieved to the particle size of 0.85–1.70 mm. The concentrations of Sr, Co, and P in each catalyst were measured in aqueous HNO_3 solutions with inductively coupled plasma (ICP) spectrometry. The incorporated catalysts are denoted as Co*xx*SrHAp, with *xx* equal to 1000Co/Sr (atomic ratio). The BET surface areas and the atomic ratio of Sr/P and Co/P of each catalyst are summarized in Table 1.

2.2. Apparatus, procedure and analysis

The catalytic experiments on the oxidation of propane and H–D exchange reaction with D_2O were performed in a fixed-bed continuous flow quartz reactor operated at atmospheric pressure. The reactor consisted of a quartz tube, 9-mm id and 35 mm in length, sealed at each end to 4-mm id quartz tubes to produce a total length of 25 cm. The catalyst charge was held in place in the enlarged portion of the reactor by two quartz wool plugs. In the oxidation of propane, prior to reaction, the catalyst was calcined in situ in an oxygen flow (25 mL/min) at 723 K for 1 h. The reaction conditions were as follows: $W = 0.5$ g, $F = 30$ mL/min, $T = 723$ K, $P(C_3H_8) = 14.5$ kPa, and $P(O_2) = 4.1$ kPa; balance to atmospheric pressure was provided by helium. The reactants and products were analyzed with an on-stream gas chromatograph (Shimadzu GC-8APT) with a TC detector and integrator. The columns used in the present study and the method employed in the calculation of the conversions and selectivities have been described previously. The reaction rates per unit of surface area were estimated as the rate ($r = FC_0X_A/W$, in which F, C_0, X_A, and W were flow rate, initial concentration of C_3H_8, conversion of C_3H_8, and catalyst weight) per catalyst surface area. In the H–D exchange reaction, the catalyst was calcined at 723 K in situ in a helium flow (15 mL/min) and then calcined in situ in an oxygen flow (25 mL/min) at 723 K for 1 h. After the calcination, the reactant gas, to which D_2O was supplied from a saturator at $P(D_2O) = 2.0$ kPa and $F = 15$ mL/min diluted by helium, was supplied to the catalyst at 723 K for 2 h. After the reaction, the reactant gas was changed to a helium flow and the temperature decreased to room temperature. H–D exchangeability of those catalysts was measured by solid state ^{1}H MAS NMR.

2.3. Characterization

The surface areas of the catalysts were calculated from adsorption isotherms obtained with a conventional BET nitrogen adsorption apparatus (Shibata P-700). X-ray photoelectron spectroscopy (XPS; Shimadzu ESCA-1000AX) used monochromatized Mg-Kα radiation. Powder X-ray diffraction (XRD) patterns were recorded with a Rigaku RINT 2500X diffractometer, using monochromatized Cu-Kα radiation. Patterns were recorded over the 2θ range of 5°–60°. The concentrations of Sr, Co, and P in each catalyst were determined in aqueous HNO_3 solution by ICP (Shimadzu ICPS-5000). ^{1}H and ^{31}P MAS NMR were obtained with a Bruker AVANCE DSX300, with an external reference of adamantane and $(NH_4)_2HPO_4$ at 1.91 and 1.33 ppm, respectively, at room temperature and a spinning rate of 25 and 4 kHz, respectively. X-ray absorption spectroscopy (XAFS) was measured (3 GeV) with a storage ring current of 67 mA at the High Energy Research Organization. The X-rays were monochromatized with channel-cut Si(311) crystals at the BL-10B station for the measurement of XAFS near the Sr K edge while those were monochromatized with a Si(111) double monochromator and the higher order harmonics were eliminated by a focusing double-mirror system at the BL-9A station for the measurement of XAFS near the Co K

edge. The absorption spectra were observed using an ionization chamber in transmittance mode. The photon energy was scanned in the range 7.4–8.8 and 15.8–17.1 keV for Co K and Sr K edges, respectively. Details of the calculation procedures on XAFS were described in our previous paper [14].

3. Results

3.1. Characterization of catalyst

XRD patterns of Co–SrHAp were essentially identical to that of SrHAp (Fig. 1) and information from Co^{2+} in Co–SrHAp was not obtained at all, although ICP and XPS analyses showed that Co is certainly present in bulk and on the surface of those catalysts (Table 1), respectively. In the XPS spectra of those fresh catalysts, peaks attributed to Sr $3p_{1/2}$, O $1s$, P $2s$, and Co $2p_{3/2}$ (when present) were found at approximately 280, 531, 190, and 782 eV, regardless of the contents of incorporated cobalt. To characterize cobalt species in the cobalt-incorporated catalysts, XAFS and ^{31}P MAS NMR have been employed. The X-ray absorption near-edge structure (XANES) spectra near the Co K edge of Co55SrHAp are shown in Fig. 2, together with that of CoO. It is evident that edge position of those samples near the Co K edge was similar, indicating that the electronic configuration of the cobalt species in Co55SrHAp is not significantly different from that of Co^{2+} in CoO. However, it should be noted that the shape of the spectra from those two samples was evidently different, indicating that the site symmetry of cobalt in those two samples was evident. Metal–oxygen distances, Sr–O and Co–O, in the nearest core obtained by EXAFS analyses of SrHAp, Co–SrHAp, and

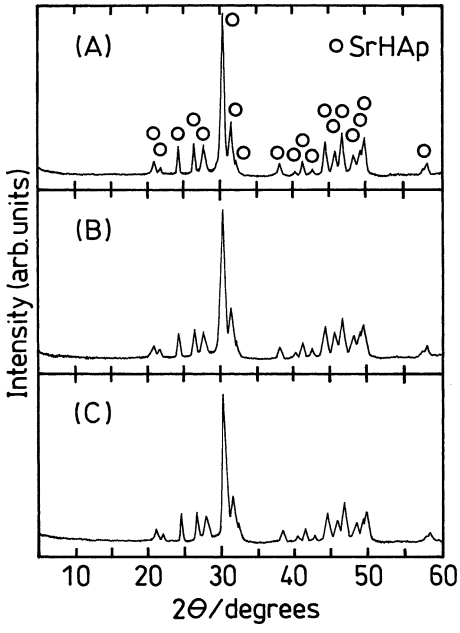

Fig. 1. XRD patterns of fresh catalysts: (A) SrHAp; (B) Co36SrHAp; (C) Co55SrHAp.

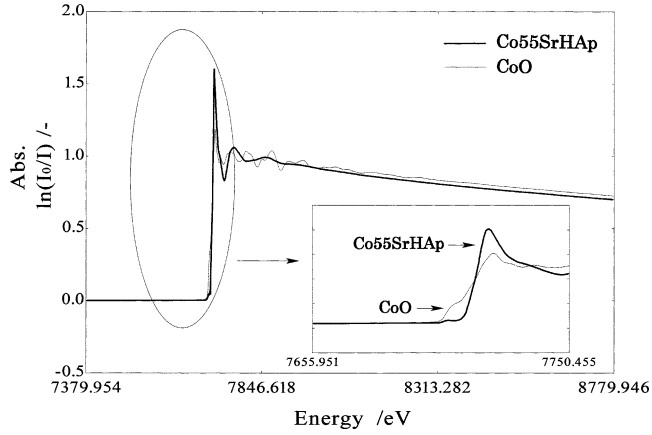

Fig. 2. XANES spectra of fresh Co55SrHAp and CoO.

CoO, are shown in Table 2. The nearest distances of Sr–O and Co–O in Co–SrHAp were insensitive to the content of Co^{2+} incorporated into SrHAp to be approximately 2.5 and 2.0 Å, respectively. It is evident that the nearest distances of Co–O in Co36SrHAp and Co55SrHAp are dissimilar to those in Co–O. ^{31}P MAS NMR spectra of SrHAp and Co–SrHAp catalysts afford indirect information on site symmetry around Co^{2+}. As shown in Fig. 3, a single ^{31}P resonance, which can be assigned to PO_4^{3-} ions in SrHAp and Co–SrHAp [8,15], was observed in the NMR spectrum. It should be noted that the intensity of the side band was greater with increasing content of Co^{2+} in Co–SrHAp.

3.2. Catalytic activities of Co–SrHAp for propane oxidation

The oxidation of propane has been examined to assess the contribution of Co species incorporated into SrHAp. With increasing incorporation of Co^{2+}, the conversion of propane, the selectivity to propylene, and the reaction rate per unit of the corresponding surface area increased as shown in Table 3 and those activities continued by 6 h on-stream. The data of Table 3 show that there is a definite improvement when Co^{2+} is added to SrHAp. However, the difference in performance between Co36SrHAp and Co55SrHAp is not impressive, particularly in the selectivity to propylene. To examine additionally the effect of the incorporation of Co^{2+} into SrHAp, Co11SrHAp was separately prepared from another lot of SrHAp, which was referred to as SrHAp-2. The conversions of propane on SrHAp-2 and Co11SrHAp were 8.2 and 11.5% while the selectivities to propylene were 38.2 and 57.0%, respectively. Therefore, it appears that

Table 2
Nearest distance of Sr–O and Co–O of fresh SrHAp and Co–SrHAp estimated by EXAFS

Sample	SrHAp	Co36SrHAp	Co55SrHAp	CoO
Sr–O (Å)	2.54	2.55	2.52	–
Co–O (Å)	–	2.04	2.01	2.45

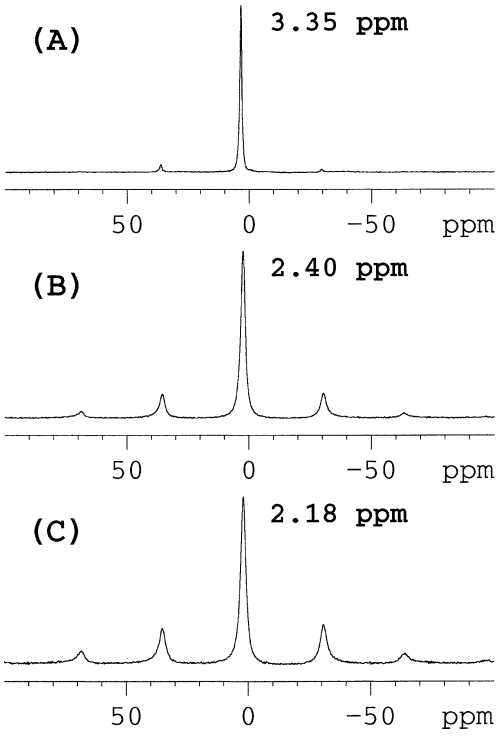

Fig. 3. ^{31}P MAS NMR of fresh catalysts: (A) SrHAp; (B) Co36SrHAp; (C) Co55SrHAp.

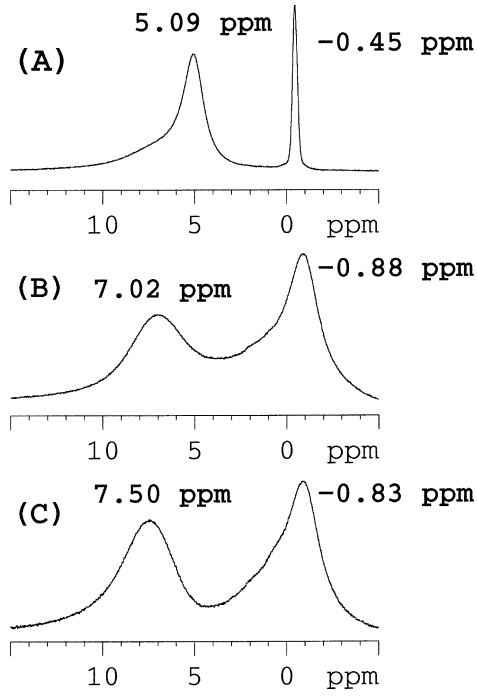

Fig. 4. ^{1}H MAS NMR of catalysts after exposure to He for 2 h at 723 K: (A) SrHAp; (B) Co36SrHAp; (C) Co55SrHAp.

the major role of Co^{2+} incorporated into SrHAp is for the enhancement of the conversion of propane.

3.3. H–D exchange of hydroxyl groups in SrHAp and Co–SrHAp with D_2O

To examine the contribution of OH^- in hydroxyapatites to hydrogen abstraction from C_3H_8, H–D exchange of OH^- ion in SrHAp and Co–SrHAp with D_2O was examined. Prior to H–D exchange reaction of SrHAp, Co36SrHAp, and Co55SrHAp with D_2O, those catalysts were treated with He for D_2O and ^{1}H MAS NMR was measured (Fig. 4). Two signals were observed from three samples, one broad signal at lower magnetic field between approximately 5.0 and 7.0 ppm due to adsorbed H_2O and the other sharp one at higher magnetic field between approximately −0.9 and −0.4 ppm due to OH^- [2,15,16]. It should be noted that, after calcination of those samples in He flow at 723 K, those samples were exposed to the atmosphere to form the absorbed H_2O. It has been reported that the corresponding ^{1}H NMR signal due to the adsorbed H_2O is observed from calcium, strontium, barium, and lead hydroxyapatites calcined in anhydrous O_2 flow but exposed to the atmosphere after the calcination [15]. As shown in Fig. 5, H–D exchange of those catalysts with D_2O resulted in a decrease of intensity of a peak at a higher magnetic field. It should be noted that the intensity of the peak decreased with increasing content of Co^{2+} in the catalysts, indicating that the introduction of Co^{2+} in the catalysts resulted in an enhancement of H–D exchange. Chemical shift obtained from ^{1}H and ^{31}P MAS NMR of SrHAp and Co–SrHAp may afford further information on the H–D exchangeability of those catalysts. Both ^{1}H and ^{31}P NMR signals obtained from

Table 3
Catalytic activities of SrHAp and Co–SrHAp for propane oxidation

Catalyst	Conversion (%)		Reaction rate[a]	Selectivity (%)				
	C_3H_8	O_2	(mol min^{-1} m^{-2})	CO	CO_2	CH_4	C_2H_4	C_3H_6
SrHAp	8.6	93	5.2×10^{-7}	23.5	47.9	–	1.6	27.0
	(8.2)	(92)	(5.0×10^{-7})	(22.6)	(47.9)	(–)	(–)	(29.5)
Co36SrHAp	17.9	79	11.4×10^{-7}	17.7	30.6	1.0	4.4	46.3
	(15.8)	(72)	(10.1×10^{-7})	(18.4)	(29.7)	(1.6)	(4.3)	(46.6)
Co55SrHAp	23.0	98	14.7×10^{-7}	13.2	32.1	1.1	5.0	48.6
	(22.1)	(98)	(14.1×10^{-7})	(14.0)	(31.4)	(1.0)	(5.0)	(48.6)

Data were collected at 0.75 and 6 h on-stream. Values in parentheses were obtained at 6 h on-stream. Reaction conditions: $T = 723$ K, $W = 0.5$ g, $P(C_3H_8) = 14.5$ kPa, $P(O_2) = 4.1$ kPa, and $F = 30$ mL/min.

[a] Reaction rates per unit of surface area.

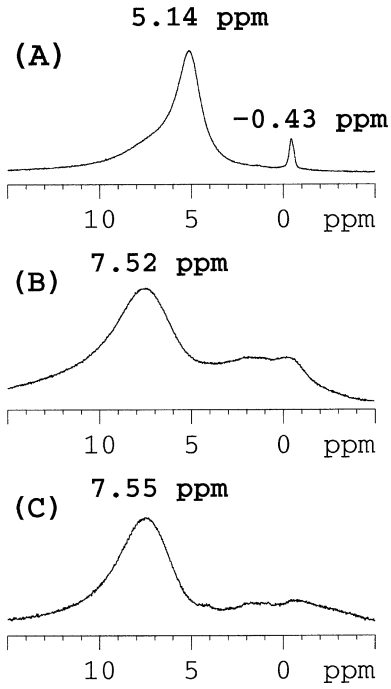

Fig. 5. ^{1}H MAS NMR of catalysts after exposure to D_2O diluted with He ($P(D_2O) = 2.0$ kPa) for 2 h at 723 K: (A) SrHAp; (B) Co36SrHAp; (C) Co55SrHAp.

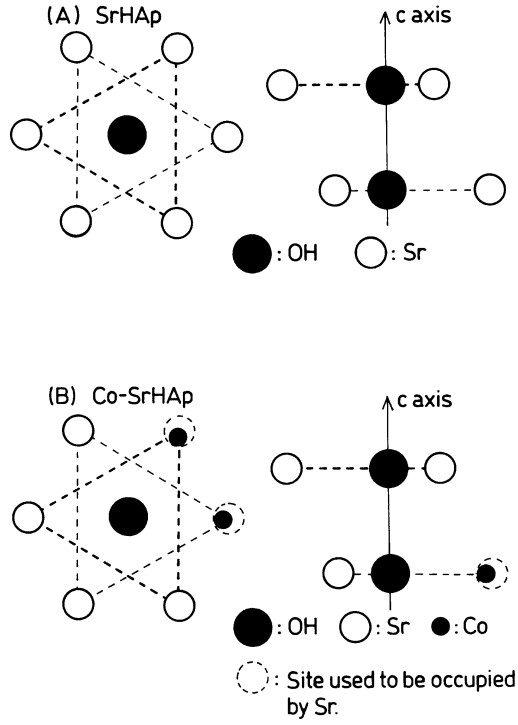

Fig. 6. Schematic illustration of local structure of SrHAp and Co–SrHAp.

the catalysts treated with He shifted to higher magnetic field, that is, from approximately −0.4 to −0.9 or −0.8 ppm and 3.4 to 2.2 ppm, respectively, with increasing Co content in the catalysts (Figs. 3 and 4). Results from ^{1}H NMR reveal that hydrogen in OH^- in Co–SrHAp becomes more anionic than that in SrHAp, resulting in favorable H–D exchange.

4. Discussion

4.1. Catalyst structure

Based on the preparation procedure of those cobalt-incorporated catalysts, three situations for cobalt species in those catalysts may be suggested: (1) ion-exchange type as $Sr_{10}(PO_4)_6(OH)_2 + Co_{10}(PO_4)_6(OH)_2$ (CoHAp); (2) solid-solution type as $Sr_{10-x}Co_x(PO_4)_6(OH)_2$; (3) Co-supported type as $CoO/Sr_{10}(PO_4)_6(OH)_2$. The results obtained by XANES (Fig. 2) and EXAFS (Table 2) indicate that Co species incorporated into SrHAp is not CoO. Therefore, the catalysts are not Co-supported type as $CoO/Sr_{10}(PO_4)_6(OH)_2$. Furthermore, a single ^{31}P MAS NMR peak was observed from Co–SrHAp, indicating that the situation for the cobalt species is not the ion-exchanged type as $Sr_{10}(PO_4)_6(OH)_2 + Co_{10}(PO_4)_6(OH)_2$ [17]. Since ^{31}P resonance of hydroxyapatite is rather sensitive to divalent cations in the apatite, two resonances due to SrHAp and CoHAp should be detected if CoHAp is formed from the incorporation of Co^{2+} into SrHAp [17]. It should be noted that the nearest distances of Sr–O in SrHAp and Co–SrHAp are longer than those of Co–O while XRD patterns of those catalysts were essentially identical. Based on these results and the structure of hydroxyapatite [18], Fig. 6 suggests the situation of cobalt in those catalysts. In Fig. 6, Sr^{2+} in SrHAp is replaced by Co^{2+} to afford Co–SrHAp as a solid-solution type of $Sr_{10-x}Co_x(PO_4)_6(OH)_2$ while the site center of those cations may be rather different. Therefore, the deviation from site symmetry of SrHAp, which can not be detected by XRD but detected by EXAFS, is produced in Co–SrHAp. The information on the site symmetry may be further obtained by ^{31}P MAS NMR (Fig. 3). A greater intensity of side band in the spectrum of Co–SrHAp indicates that site symmetry around P species may fall into disorder due to site positioning of Co^{2+}. Only one ^{31}P MAS NMR peak from SrHAp and Co–SrHAp demonstrates that PO_4^{3-} ions in both unit cells have a similar structural environment, suggesting the formation of solid solution like $Sr_{10-x}Co_x(PO_4)_6(OH)_2$ from the incorporation of Co^{2+} into SrHAp.

4.2. Advantageous effects of the incorporation of Co^{2+} in SrHAp

As shown in Table 3, the advantageous effects of the incorporation of Co^{2+} into SrHAp are evident. The employment of Co compounds as a catalyst for the oxidation of propane has been reported from several groups [19–24] and an advantageous influence of the incorporation of Co species into molybdates [20–24] and tungstates [23] has been reported to the oxidative dehydrogenation of propane. It should be noted that those catalysts are oxides, indi-

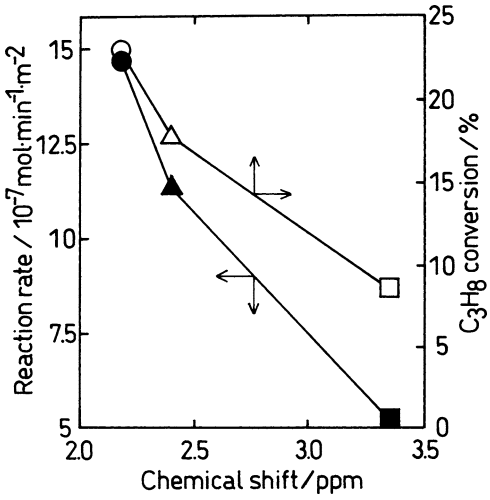

Fig. 7. Dependence of C_3H_8 conversion and reaction rate on chemical shift from ^{31}P MAS NMR. Symbols: circle, Co55SrHAp; triangle, Co36SrHAp; and square, SrHAp. Open symbols: for C_3H_8 conversion. Closed symbols: for reaction rate.

cating that hydrogen abstraction from C_3H_8 to C_3H_6 proceeds on lattice oxygen [25]. In hydroxyapatite, two oxygen species, PO_4^{3-} and OH^-, are present. Since it already has been reported that the activities of calcium hydroxyapatite ($Ca_{10}(PO_4)_6(OH)_2$) for the oxidation of C_3H_8 is evidently greater than those of $Ca_3(PO_4)_2$ [26], the phosphate groups do not directly contribute to hydrogen abstraction from the alkane.

4.3. Role of hydroxyl groups in hydroxyapatites

Although it is rather strange that OH^- groups in the catalysts directly contribute to hydrogen abstraction from C_3H_8, OH^- groups may be a source of active oxygen species. If H–D exchange proceeds favorably with increasing Co content in the catalysts at the reaction temperature employed in propane oxidation, it may be suggested that it is easy for hydrogen in hydroxyl groups to be removed from OH^- to produce an active oxygen species like lattice oxygen on the Co-rich catalysts. It should be noted that this does not reveal that the active oxygen species is stably present during propane oxidation since the active oxygen species should be recombined with hydrogen or deuterium. This means that a probability of the presence of the active oxygen species during propane oxidation is enhanced on the Co-rich catalysts. Since the activities for the oxidation of propane and those of H–D exchangeability were evidently enhanced with increasing Co^{2+} content in the catalysts, the above speculation may be acceptable, although no direct and solid evidence for the presence of such oxygen species can not be revealed in the present study. Since PO_4^{3-} does not directly bond to OH^-, it is impossible to discuss as done with ^{1}H NMR; it is worthwhile to mention that relationship between the conversion of propane and ^{31}P chemical shift from those catalysts was evidently observed as shown in Fig. 7.

5. Conclusion

1. Based on the results obtained by XRD, ^{31}P MAS NMR, and XAFS, the structure of strontium hydroxyapatite incorporated with cobalt was suggested to be a solid-solution type, $Sr_{10-x}Co_x(PO_4)_6(OH)_2$.
2. The catalytic activities for the oxidative dehydrogenation of propane on SrHAp and Co–SrHAp were enhanced with increasing content of cobalt in the catalysts.
3. H–D exchangeability of SrHAp and Co–SrHAp was also enhanced with increasing the content of cobalt in the catalysts.
4. It was suggested that a probability of the presence of the active oxygen species during propane oxidation is enhanced on the Co-rich catalysts, resulting in the enhancement of the catalytic activities for the oxidative dehydrogenation of propane on Co-rich catalysts.

Acknowledgments

This work was partly funded by a Grant-in-Aid for Scientific Research on Priority Areas (KAKENHI 13126215) to H.H. from the Ministry of Education, Culture, Sports, Science and Technology (MEXT) and a Grant-in-Aid for Scientific Research (C) (KAKENHI 14550801) to S.S. from the Japan Society for the Promotion Science (JSPS), to which our thanks are due. This work has been performed under the approval of the Photon Factory Advisory Committee (Proposal No. 2001G090).

References

[1] D.E.C. Corbridge, Studies in Inorganic Chemiastry 10, Phosphorous, An Outline of its Chemistry, Biochemistry and Technology, 4th ed., Elsevier, Amsterdam, 1990.
[2] J.C. Elliott, Structure and Chemistry of the Apatites and Other Calcium Orthophosphates, Elsevier, Amsterdam, 1994.
[3] S. Sugiyama, T. Minami, H. Hayashi, M. Tanaka, N. Shigemoto, J.B. Moffat, J. Chem. Soc. Faraday Trans. 92 (1996) 293.
[4] S. Sugiyama, T. Minami, T. Higaki, H. Hayashi, J.B. Moffat, Ind. Eng. Chem. Res. 36 (1997) 328.
[5] S. Sugiyama, Y. Fujii, K. Abe, H. Hayashi, J.B. Moffat, Energy Fuels 13 (1999) 637.
[6] S. Sugiyama, Y. Iguchi, H. Nishioka, T. Minami, T. Moriga, H. Hayashi, J.B. Moffat, J. Catal. 176 (1998) 25.
[7] S. Sugiyama, T. Shono, E. Nitta, H. Hayashi, Appl. Catal. A 211 (2001) 123.
[8] J.A.S. Bett, L.G. Christner, W.K. Hall, J. Am. Chem. Soc. 89 (1967) 5535.
[9] N.W. Cant, J.A.S. Bett, G.R. Wilson, W.K. Hall, Spectrochim. Acta A 27 (1971) 425.
[10] T. Ishikawa, Stud. Surf. Sci. Catal. 99 (1996) 301.
[11] S. Sugiyama, J.B. Moffat, Catal. Lett. 76 (2001) 75.
[12] S. Sugiyama, J.B. Moffat, Catal. Lett. 81 (2002) 77.
[13] Y. Amenomiya, V.I. Birss, M. Goledzinowski, J. Galuszka, A.R. Sanger, Catal. Rev.–Sci. Eng. 32 (1990) 163.

[14] S. Sugiyama, T. Moriga, M. Goda, H. Hayashi, J.B. Moffat, J. Chem. Soc. Faraday Trans. 92 (1996) 4305.
[15] S. Sugiyama, T. Moriga, H. Hayashi, J.B. Moffat, Bull. Chem. Soc. Jpn. 74 (2001) 187.
[16] J.P. Yesinowski, H. Eckert, J. Am. Chem. Soc. 109 (1987) 6274.
[17] S. Sugiyama, S. Hayashi, H. Hayashi, T. Tomida, Phosphorus Res. Bull. 12 (2001) 53.
[18] M.I. Kay, R.A. Young, A.S. Posner, Nature 204 (1964) 1050.
[19] Y. Takita, H. Yamashita, K. Moritaka, Chem. Lett. (1989) 1733.
[20] Y.-S. Yoon, N. Fujikawa, W. Ueda, Y. Moro-oka, K.-W. Lee, Catal. Today 24 (1995) 327.
[21] D.L. Stern, R.K. Grasselli, J. Catal. 167 (1997) 550.
[22] D.L. Stern, R.K. Grasselli, J. Catal. 167 (1997) 560.
[23] D.L. Stern, R.K. Grasselli, J. Catal. 167 (1997) 570.
[24] M. Okamoto, L. Luo, J.A. Labinger, M.E. Davis, J. Catal. 192 (2000) 128.
[25] Y. Takita, Shokubai (Catal. Catak.) 38 (1996) 143.
[26] S. Sugiyama, E. Nitta, H. Hayashi, J.B. Moffat, Catal. Lett. 59 (1999) 67.